JOURNAL OF MATERIALS SCIENCE 32 (1997) 2163–2170

# Mechanical performance of the extruded blends of liquid-crystalline copolyester and modified polyphenylene oxide

S. C. TJONG, S. L. LIU R. K. Y. LI
*Department of Physics and Materials Science, City University of Hong Kong, 83 Tat Chee Avenue, Kowloon, Hong Kong*

Polymer blends of modified polyphenylene oxide (PPO) and thermotropic polyester were prepared by extrusion followed by drawing. The morphology and mechanical properties of the blends were examined by scanning electron microscopy, static tensile tests and dynamic mechanical analysis. The static mechanical tests showed that the liquid-crystalline polymers (LCP) additions led to an increase in both modulus and tensile strength of the blends, while elongation at break was generally decreased. The magnitude of the reinforcing effect depended significantly on the LCP content, but also on draw ratio. The Tsai–Halpin equation was used to estimate the aspect ratio of LCP microfibrils. The storage modulus showed that the LCP phase tended to reinforce the PPO matrix over a wide range of temperature but not near the glass transition zone.

## 1. Introduction

Recently, polymer blends of thermotropic liquid-crystalline polymers (LCPs) with isotropic polymers have attracted considerable attention because of the potential for producing high-performance polymeric materials. LCPs usually consist of rod-like molecular chains and can be shaped into highly oriented structures by means of the usual processing techniques. LCPs generally exhibit lower viscosities than isotropic polymer melts, and there can be an improved processability for the polyblends. Furthermore, the dispersed LCP phase is deformed into a fibrillar structure during processing, acting as a reinforcing phase. Thus the mechanical properties of some thermoplastics can be enhanced by the addition of a small amount of LCP. The morphology and physical properties of these thermoplastic/LCP blends are similar to those of conventional short-fibre-reinforced plastics [1].

The thermoplastic/LCP blends are mainly incompatible and immiscible. The dispersed LCP phase exhibits spherical, ellipsoidal or fibrillar structures. The degree of orientation of the LCP fibrils can be modified through choice of processing conditions, especially by applying elongational or shear forces to the molten polymer. Extensional flow is known to be more effective than shear flow in producing materials with a high degree of molecular orientation [2, 3]. Increased orientation of the LCP fibrils by additional drawing can greatly improve the mechanical properties of the thermoplastic/LCP blends [4–8]. Furthermore, there exists some parameters affecting the LCP phase morphology such as the viscosity ratio of the LCP and thermoplastics, the LCP concentration, etc. [9–14]. In this study, the morphology structure and mechanical properties of extruded modified PPO/LCP blends were investigated by means of scanning electron microscopy (SEM), dynamic mechanical analysis (DMA), and static tensile tests. The thermoplastic matrix is a blend of poly-2, 6-dimethyl-1, 4-phenylene oxide (PPO) with polystyrene (PS). Pure PPO exhibits a high glass transition temperature, excellent tensile strength, good chemical resistance but poor processability [15]. However, PS is an extremely brittle polymer. Blending of PPO with PS produces a tough material with good processability. The PPO is sold commercially blended with PS as the PPO/PS blends are compatible at all compositions on the basis of DSC [16–18] and DMA analyses [19]. The mechanical and thermal properties of the pure PPO/LCP blends have been investigated by some workers [20, 21]. Limtasiri and Isayev [20] reported that the mechanical properties of the injection-moulded PPO/LCP blends were found to be slightly improved at low LCP and dramatically improved at above 50% LCP contents. In addition, impact strength was significantly increased up to two times, after adding 10% LCP into the matrix. On the other hand, Crevecoeur and Groeninckx [4] have investigated the morphology and mechanical properties of the injection-moulded and fibre-spun PPO/PS blends containing LCP additions. They indicated that the mechanical properties of the injection-moulded blends are below predictions of the rule of mixtures because the LCP is only moderately elongated into fibrils. However, fine fibrils with nearly infinite aspect ratio are formed in the fibre-spun samples. In this case, the modulus tends to increase linearly with the LCP

0022–2461  

volume fraction [4]. The present work places emphasis on the morphology and mechanical properties of the modified PPO/LCP blends extruded at different draw ratios. The purpose was to determine the correlation between the mechanical properties with materials internal morphology.

## 2. Experimental procedure

The matrix polymer used in this work was modified PPO resin (Noryl PX 1214-710). PPO is a registered trademark of the General Electric Co. The thermotropic liquid-crystalline polymer used was Vectra A950 produced by Hoechst-Celanese. Vectra A950 is a copolyester of 75 mol% *p*-hydroxybenzoic acid (HBA) and 25 mol % 2, 6-hydroxynaphthoic acid (HNA), which exhibits a nematic mesophase in the molten state.

Before blending, the LCP and modified PPO were separately dried in the ovens. Blends of LCP composition ranging from 5–50 wt % were prepared at 290 °C using a twin-screw extruder (Brabender Plasticorder). A ribbon die of $50 \times 0.5\,mm^2$ was attached to the extruder. The extrusion was followed by drawing the extruded melt directly with a take-up machine, with the draw ratio being varied by changing the speed of the machine. The draw ratio (DR) was determined from the cross-sectional areas of the die, and the extruded strand measured by an optical microscope.

The static mechanical properties were obtained using an Instron tensile machine at room temperature and at a crosshead speed of $1\,mm\,min^{-1}$. Each tensile property was averaged over six tests. Dynamic mechanical measurements were carried out using a Du Pont dynamic mechanical analyser (model 983) at

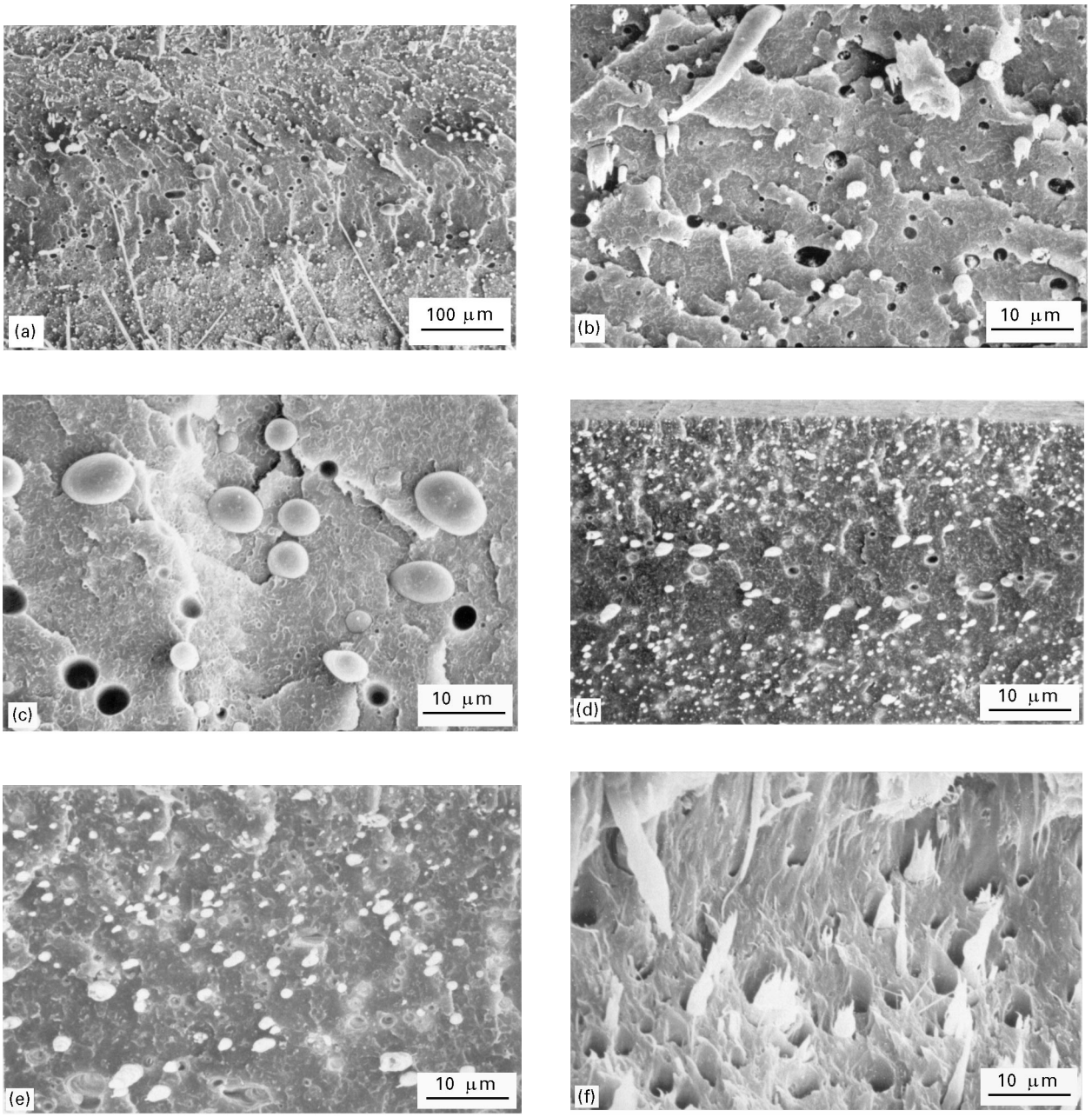


*Figure 1* Scanning electron micrographs of the PPO/10 LCP blend prepared at (a) a draw ratio of 1.5, low magnification, showing the entire fracture surface, (b) a draw ratio of 1.5, higher magnification of the edge region, (c) a draw ratio of 1.5, higher magnification of the core region, (d) a draw ratio of 4.1, low magnification, (e) a draw ratio of 4.1, higher magnification of the edge region, and (f) a draw ratio of 7.9.

a fixed frequency of 1 Hz and an oscillation amplitude of 0.2 mm. The temperature range of study was from $-100$ to 150 °C and the heating rate employed was 3 °C $min^{-1}$.

A scanning electron microscope (Jeol JSM 820) was used to examine the morphology of the extruded ribbons. The ribbons were broken in liquid nitrogen, perpendicular to the flow direction. The fracture surfaces were coated with gold prior to SEM observations.

## 3. Results and discussion

### 3.1. Morphology

Fig. 1a–1f show scanning electron micrographs of the fracture surfaces of the PPO/10 LCP strands of different draw ratios. A clear skin–core structure is observed in this blend for some draw ratios. At a fixed draw ratio of 1.5, the thickness of the skin layer is $\sim 170$ μm. At this smaller LCP addition, only few LCP domains are elongated to microfibrils in the skin region (Fig. 1b). Most of the LCP domains protrude little from the matrix. Furthermore, microvoids are readily observed in this micrograph indicating that the adhesion between the LCP dispersed phase and the modified PPO is relatively poor. Near the core region, the LCP domains are in spherical form (Fig. 1c). As the draw ratio is increased to 4.1, the thickness of the skin layer appears to increase slightly (Fig. 1d). The LCP domains are slightly elongated and the microfibrils formed are not well developed (Fig. 1e). However, better fibril formation and orientation of the LCP phase can be achieved by increasing the draw ratio to 7.9 (Fig. 1f).

Fig. 2a–d show scanning electron micrographs of the fracture surface of the PPO/20 LCP strands. Apparently, the LCP microfibrils produced exhibit a larger aspect ratio with increasing LCP concentration (Fig 2b). At a higher draw ratio of 7.9, there are abundant fibrils throughout the strand, and the LCP fibrils are also observed in the core region (Fig. 2d). It is generally known that fibrillation of the LCP dispersed phase is favoured by the elongation flow during the drawing process. The aspect ratio of a microfibril becomes larger as the elongation flow field becomes stronger [22]. In *in-situ* composite blends, the orientation and aspect ratio of the LCP fibrils are decisive factors for the improvement in Young's modulus and tensile strength. At 40 wt % LCP, long LCP fibrils are developed in the skin region even at a small draw ratio of 1.5 (Fig. 3a). In the core region, the LCP domains are deformed into ellipsoids (Fig. 3b). However, extensive LCP fibril formation is observed in the entire strand as the draw ratio is increased to 4.1 and above (Fig. 3c and d).

### 3.2. Static mechanical properties

Fig. 4a shows the tensile strength of the blends investigated versus LCP content. The variation of tensile strength with draw ratio for PPO/LCP strands is shown in Fig. 4b. From Fig. 4a, the ultimate strength of the blends appears to increase with increasing LCP content as expected. Improvement of tensile strength

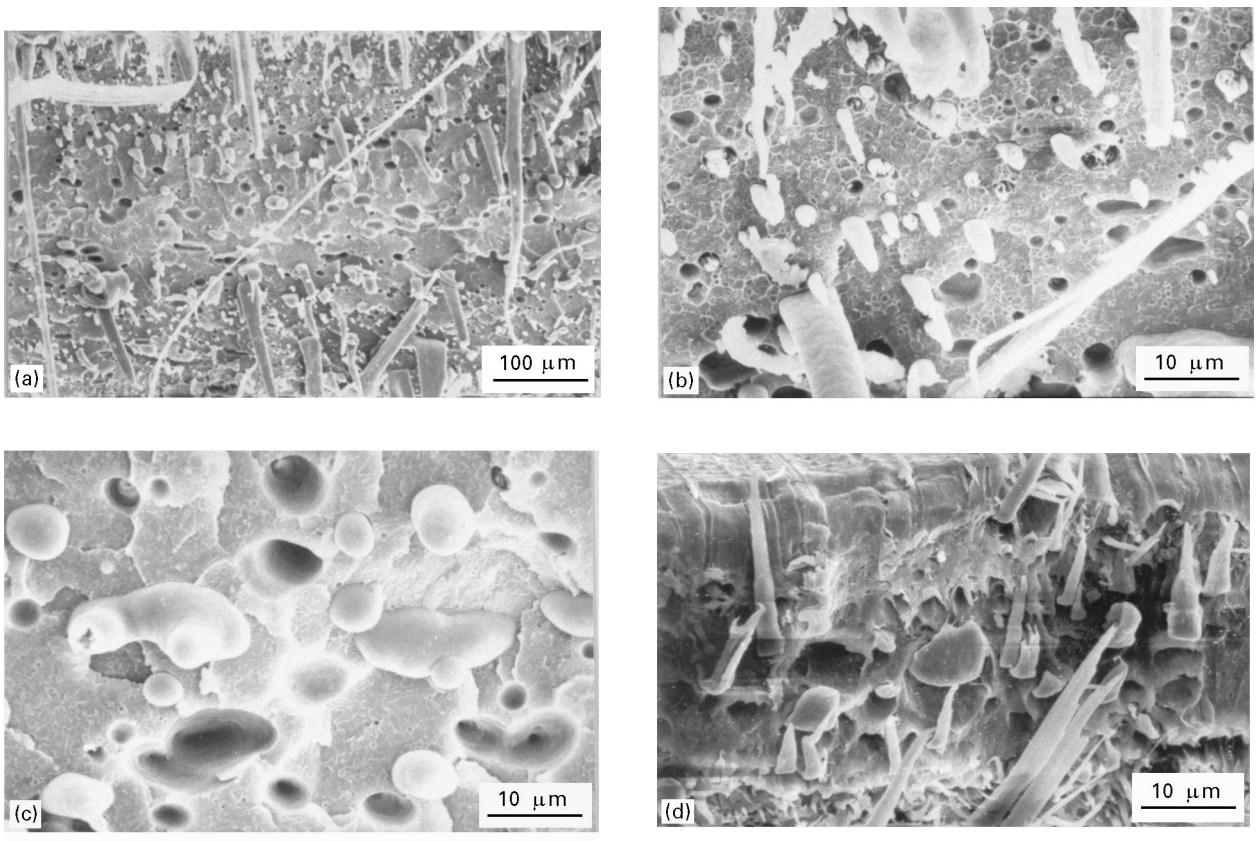


*Figure 2* Scanning electron micrographs of the PPO/20LCP blend prepared at (a) a draw ratio of 1.5, low magnification, showing the entire fracture surface, (b) a draw ratio of 1.5, higher magnification of the edge region, (c) a draw ratio of 1.5, higher magnification of the core region and (d) a draw ratio of 7.9, showing the entire fracture surface.

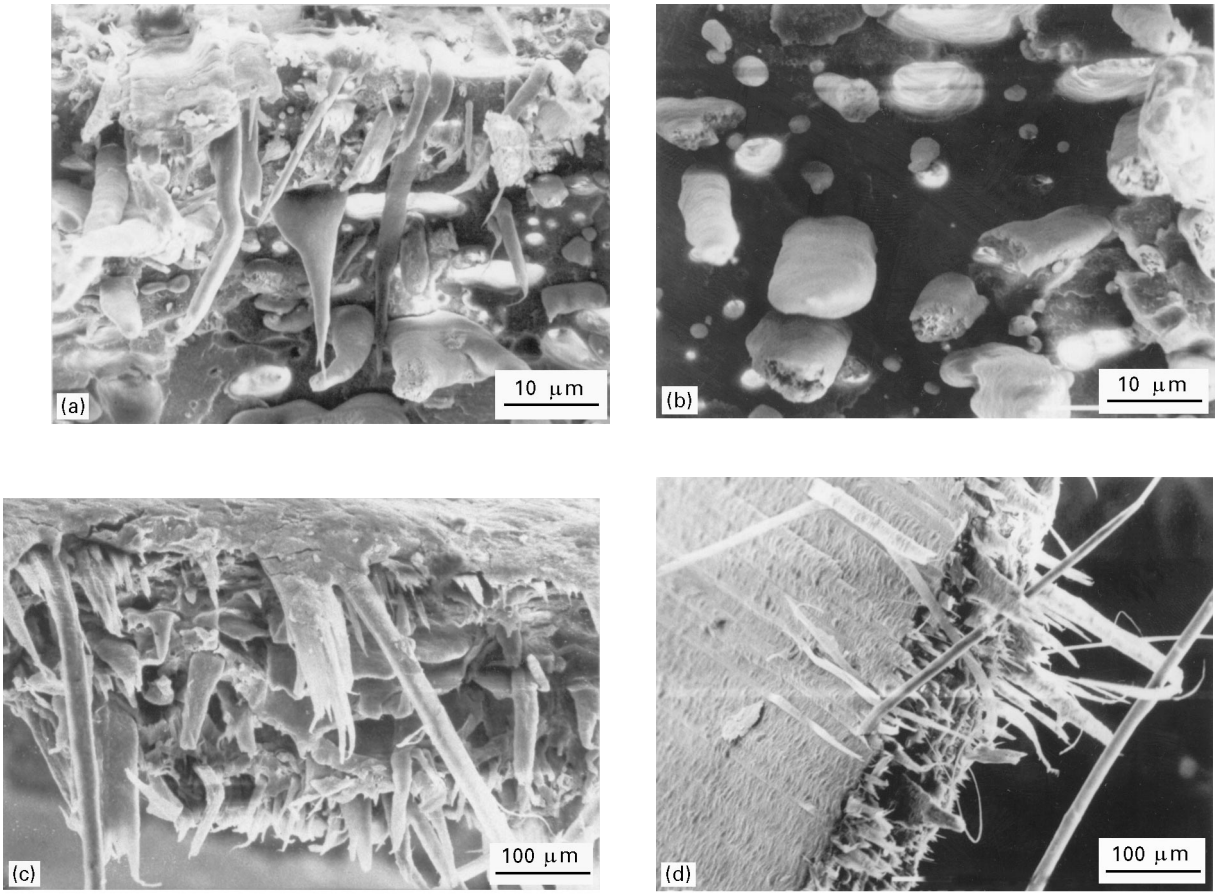


*Figure 3* Scanning electron micrographs of the PPO/40LCP blend prepared at (a) a draw ratio of 1.5, (b) a draw ratio of 1.5, higher magnification of core region, (c) a draw ratio of 4.1, showing the entire fracture surface and (d) a draw ratio of 7.9, showing the entire fracture surface.

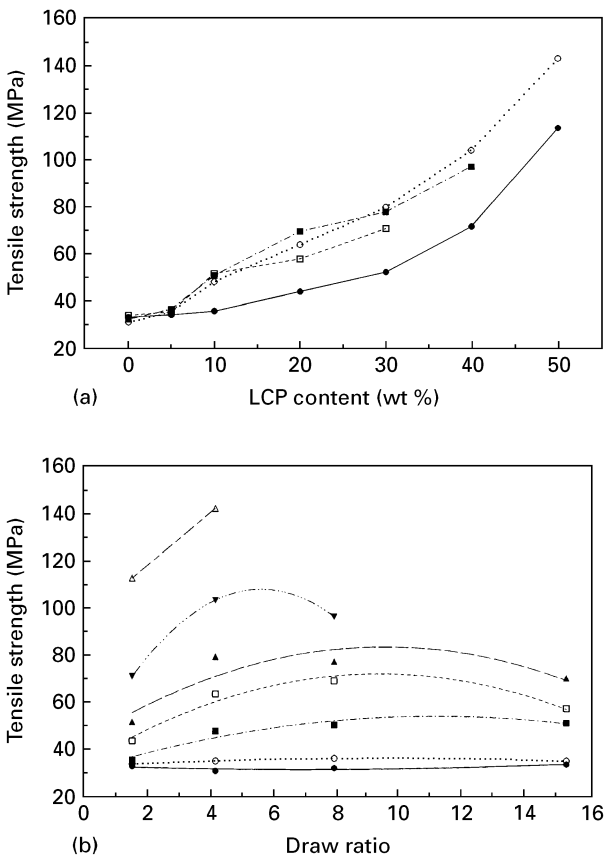


*Figure 4* Tensile strength versus (a) LCP content of PPO/LCP blends, and (b) a draw ratio for PPO/LCP blends. (a) DR = (●) 1.5, (○) 4.1, (■) 7.9, (□) 15.2; (b) LCP content = (●) 0%, (○) 5%, (■) 10%, (□) 20%, (▲) 30%, (▼) 40%, (△) 50%.

of the PPO/LCP blends with increasing LCP content and draw ratio is due to the formation of long LCP fibrils, as verified by the scanning electron micrographs.

Fig. 5a shows the variation of tensile modulus versus LCP content. It is evident that the elastic modulus increases monotonically with increasing LCP content and draw ratio. For the PPO/30 LCP blend, increasing the draw ratio from 1.5 to 15.2 leads to a 109% improvement in modulus. The variation of tensile modulus with draw ratio is shown in Fig. 5b. The tensile modulus increases considerably at low draw ratio but it levels off after a certain value of draw ratio. Such behaviour has also been observed in other thermoplastic/LCP blends [4, 23]. Crevecoeur and Groeninckx [4] suggested that maximum elongation and orientation of the LCP are reached after a certain draw ratio; further drawing does not result in an improvement of mechanical properties. Lee *et al.* [23] reported that there exists an apparent dependence of the modulus on the draw ratio. They also indicated that the formation of LCP fibrils does not take place entirely before and in the die, but it also takes place beyond the die exit in the drawing process. The orientation of the nematic phase varies from highly oriented at the walls to much less oriented at the centre of the extruder. As the melt is hot drawn in an extensional flow field, the nematic domains are drawn into oriented fibrils of high aspect ratio [23]. These results indicate that the elastic modulus can be markedly improved by drawing as the aspect ratio of

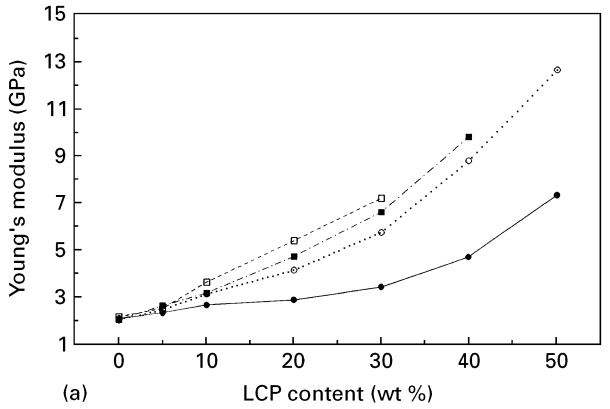


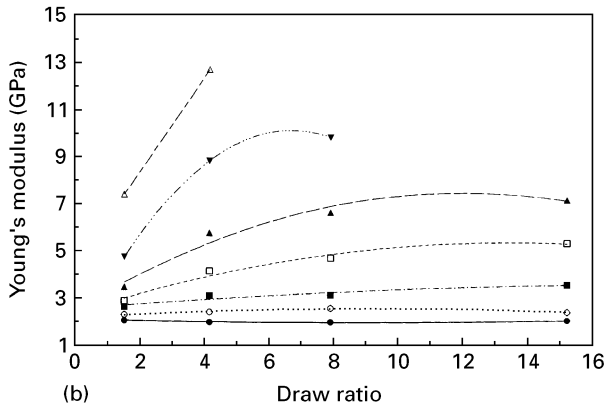


*Figure 5* Tensile modulus versus (a) LCP content for PPO/LCP blends and (b) draw ratio for PPO/LCP blends. (a) DR = (●) 1.5, (○) 4.1, (■) 7.9, (□) 15.2; (b) LCP content = (●) 0%, (○) 5%, (■) 10%, (□) 20%, (▲) 30%, (▼) 40%, (△) 50%.

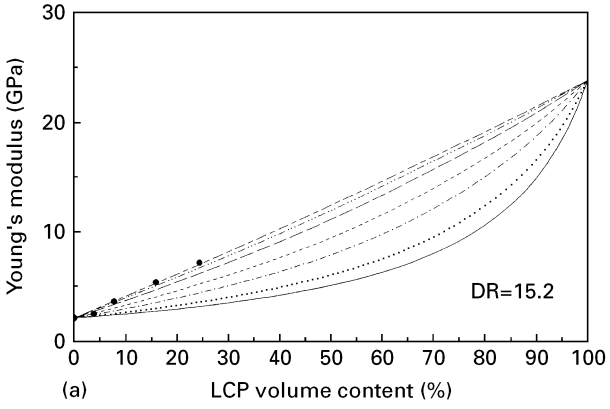


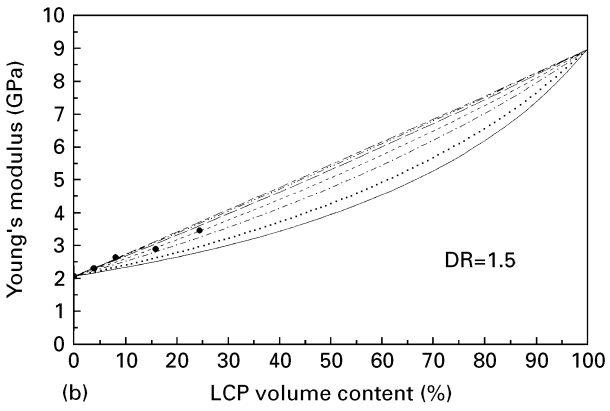


*Figure 6* Graphical representation of the Tsai–Halpin equation at (a) a draw ratio of 15.2 and (b) a draw ratio of 1.5. Aspect ratios are indicated in the figure. AS: (——) 1, (· · ·) 2, (— · —) 5, (– – –) 10, (— — —) 25, (— - - - —) 50, (———–———) 100, (●) experimental data.

the LCP microfibres is increased. The aspect ratio of the LCP fibres is generally difficult to determine. It can be estimated from the Tsai–Halpin equation modified by Nielson [24, 25], as long as the fibres are discontinuous and are aligned uniaxially. The elastic modulus of short-fibre-reinforced composites $E_c$, is given by

$$\frac{E_c}{E_m} = \frac{1 + \xi\eta V_f}{1 - \eta V_f} \tag{1}$$

where $E_m$ is the tensile modulus of the matrix and $V_f$ is the volume fraction of fibre reinforcement. The constant $\xi$ and $\eta$ are given by

$$\xi = 2(L/D) \tag{2}$$

$$\eta = \frac{(E_f/E_m) - 1}{(E_f/E_m) + \xi} \tag{3}$$

where $L/D$ is the aspect ratio (length/diameter) of the reinforcing fibres, and $E_f$ is the modulus of the fibre. The constant $\xi$ can be obtained by selecting an appropriate value for the best fit plot of $E_c/E_m$ versus $V_f$.

Fig 6a shows a typical graphic representation of the Tsai–Halpin equation with different aspect ratios at a draw ratio of 15.2. The moduli of the matrix of PPO and LCP were measured to be 2.06 and 23.93 GPa, respectively. The measured modulus for LCP fibres in the composite is assumed to be comparable to its value extruded neat with a similar draw ratio. However, the fibre-spun Vectra has been reported to have a modulus of 45 GPa at a spin–draw ratio of about 30 [26]. This higher value of melt-spun fibres is due to the fact that the effect of the skin–core morphology is reduced dramatically because the fibre consists of highly uniaxial material. Lin and Yee [27] also indicated that the elastic modulus of LCP fibres is expected to change with draw ratio due to the molecular orientation of the LCP reinforcing phase increasing with drawing. From Fig. 6a, the experimental values appear to have a large aspect ratio for the PPO/LCP blends containing up to 24.3 vol % LCP. The aspect ratio (AS) defines the ratio of the length over the diameter of the fibril. A graphic representation of the Tsai–Halpin equation for the PPO/LCP blends made at a draw ratio of 1.5 is shown in Fig. 6b. In this case, the aspect ratio of LCP fibre for the extruded PPO/LCP blends made at a draw ratio of 1.5 appears to be considerably lower than that as shown in Fig. 6a. It is possible to relate the aspect ratio determined from the Tsai–Halpin equation with that estimated from the optical micrograph. For example, the aspect ratio determined from Tsai–Halpin equation for the PPO/LCP blend containing 24.3 vol % LCP drawn at a ratio of 1.5, is 10. A rough estimation of the aspect ratio of the fibril formed in this sample as shown in Fig. 7 is about 15. From the optical micrograph as shown in Fig. 7, some fibrils are debonded from the polymer matrix due to polishing. Furthermore, one can also observe the formation of deep

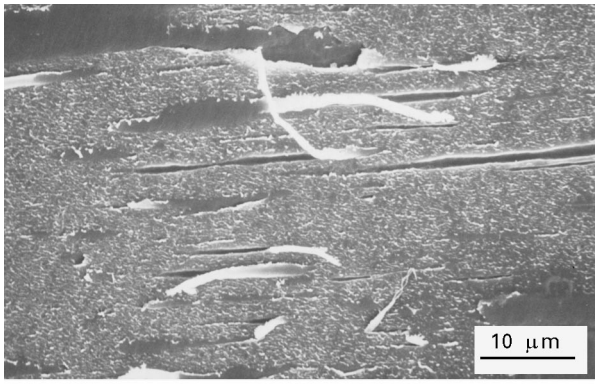


*Figure 7* Optical micrograph of the PPO/24.3 vol % LCP blend drawn at a ratio of 1.5. The sample was mounted in epoxy followed by polishing.

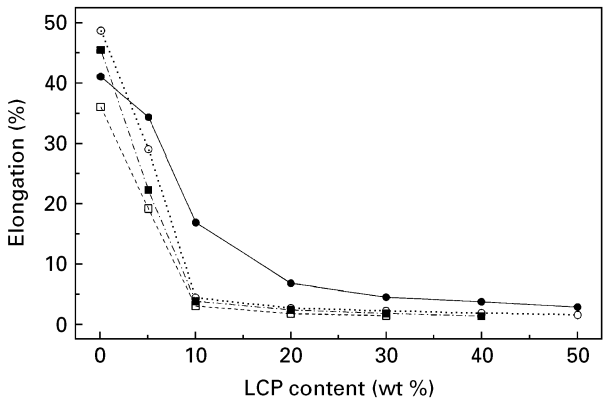


*Figure 8* Elongation at break versus LCP content for PPO/LCP blends at various draw ratios: (●) 1.5, (○) 4.1, (■) 7.9, (□) 15.2.

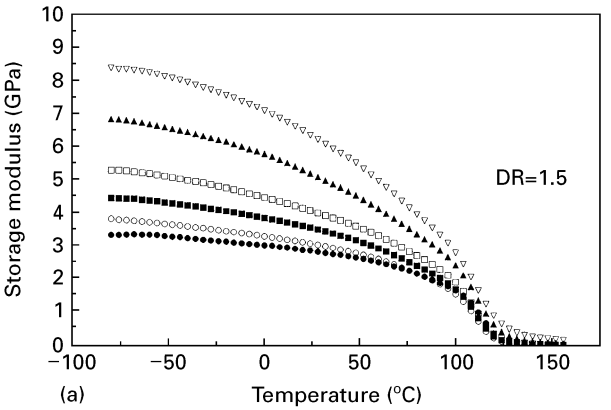


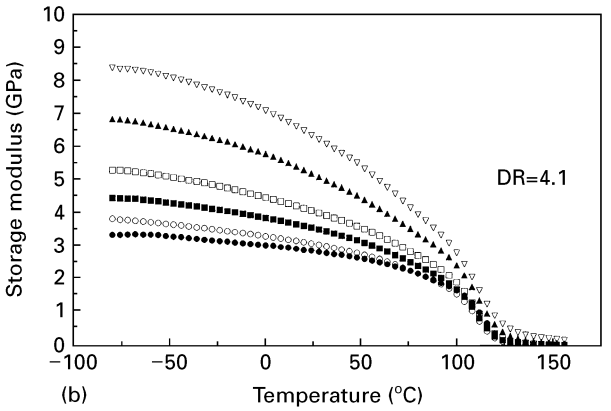


*Figure 9* Storage modulus versus temperature for the PPO/LCP blends prepared at (a) a draw ratio of 1.5 and (b) a draw ratio of 4.1. LCP content: (●) 0%, (○) 10%, (■) 20%, (□) 30%, (▲) 40%, (▽) 50%.

grooves associated with the complete removal of the fibrils from the polymer matrix. The aspect ratio is approximately determined from the average value of the length of the fibril and the groove divided by the diameter of the fibril. Thus a good correlation is obtained for the aspect ratio determined from the Tsai–Halpin equation and that estimated from the optical micrograph.

Fig. 8 shows the typical elongation at break of the blends as a function of the LCP concentration. The modified PPO exhibits ductile behaviour due to its large value of elongation at break. However, it is apparent in this figure that the LCP additions lead to a drastic reduction in the ductility of PPO. Moreover, the elongation at break of the blends appears to decrease with increasing draw ratio. At a draw ratio of 4.1 and above, the addition of 10 wt % LCP transforms the ductile characteristics to brittle behaviour.

## 3.3. Dynamic mechanical properties

Fig. 9a and b show typical variation of storage modulus of PPO/LCP blends versus LCP contents at draw ratios of 1.5 and 4.1, respectively. At a fixed draw ratio of 1.5, the storage modulus appears to increase with increasing LCP concentrations. The improvements in modulus is observed for a wide range of temperatures scanned except near the glass transition temperature, $T_g$. The onset of the glass transition is accompanied by a drop in storage modulus. Similar behaviour is observed in the extruded PPO/LCP blends made at a draw ratio of 4.5. Thus the LCP dispersed phase reinforces the PPO matrix effectively. Furthermore, the storage modulus at room temperature shows almost the same tendency with the elastic modulus obtained from the static tensile tests, i.e. it tends to increase with increasing LCP contents. However, Turek *et al.* [21] reported that the dynamic mechanical storage modulus of LCP/PPO blends decreases with increasing LCP contents over the wide temperature range, except at room temperature. In other words, the LCP reinforces the PPO matrix at room temperature only. At higher temperatures, the modulus of the blend becomes dominated by the stiffness of the PPO phase, which essentially reinforces the LCP material. They attributed this to the constant, steady decrease in the storage modulus of LCP (Vectra A950) with temperature. The PPO used in their work is assumed to be of high purity on the basis of the high glass transition temperature observed, i. e. 212 °C [21]. Our DMA results do not agree with those reported by Turek *et al.* [21], and this difference possibly arises because a higher modulus neat PPO was used in their study.

Fig. 10a and b show the loss factor versus temperature for the PPO/LCP blends at draw ratios of 1.5 and 4.1, respectively. The $T_g$ of modified PPO is

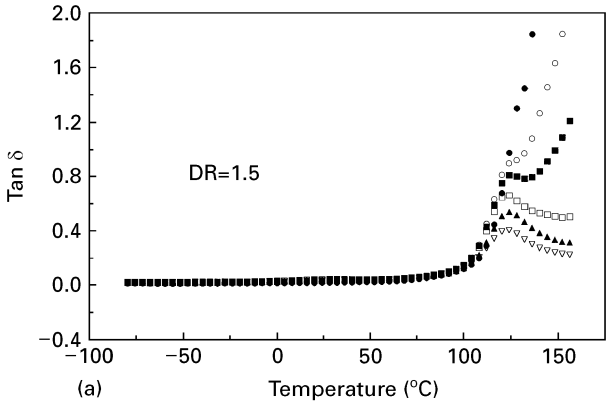


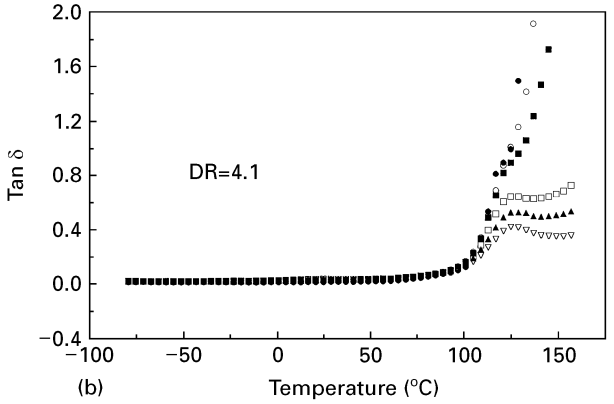


*Figure 10* Tan δ versus temperature for the PPO/LCP blends prepared at (a) a draw ratio of 1.5 and (b) a draw ratio of 4.1. LCP content: (●) 0%, (○) 10%, (■) 20%, (□) 30%, (▲) 40%, (▽) 50%.

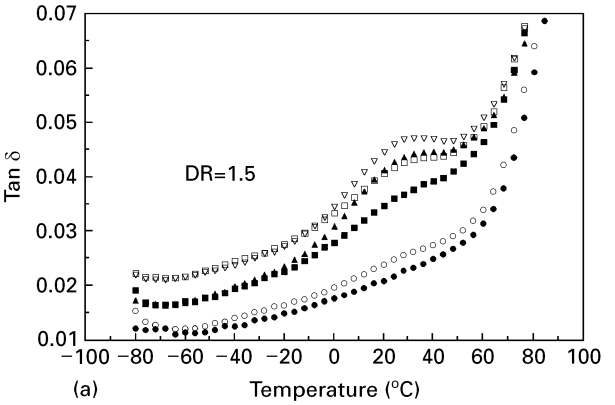


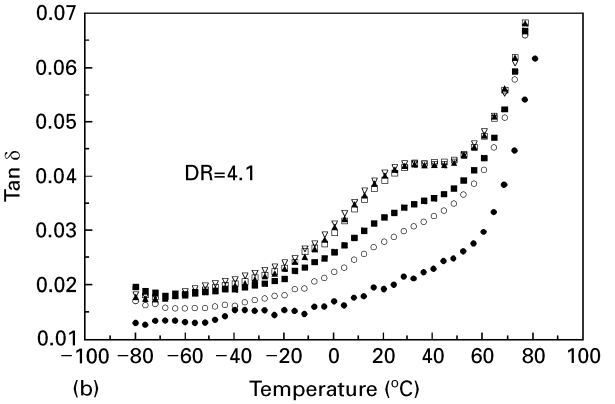


*Figure 11* Tan δ versus temperature for the PPO/LCP blends in the temperature range − 100 to 100 °C. The blends were prepared at (a) a draw ratio of 1.5 and (b) a draw ratio of 4.1. LCP content: (●) 0%, (○) 10%, (■) 20%, (□) 30%, (▲) 40%, (▽) 50%.

located at ~ 123 °C. The $T_g$ of modified PPO is much lower compared to that of pure PPO [21]. This is attributed to the incorporation of polystyrenes in the polymeric matrix. The composition ratio between the PPO and PS in Noryl used in this work was not given by General Electric. However, Tenkkanat and Gibala [28] have determined the $T_g$s of a series of PS–PPO blends using differential scanning calorimetry [28]. They indicated that $T_g$ of the 75 PS–25 PPO (wt %) blend is located at 122 °C. As the $T_g s$ of PS and pure PPO are 110 and 210 °C, respectively, it is reasonable to assume that the Noryl used in this work contains a relatively high concentration of PS and a low content of PPO.

It has been reported previously that the loss factor spectrum of Vectra A950 exhibits a broad peak at ~ 40 °C and a rather sharp peak at 110 °C which are designated as the β and α relaxations, respectively [29, 30]. Troughton *et al.* [31] reported that the α relaxation corresponds to the materials changing from a glassy state to a mobile nematic phase, whereas the β relation is associated with the motion of the naphthalene rings. Blundell and Buckingham [29] indicated that the naphthalene motions are strongly coordinated with any carbonyl group that is an immediate neighbour, such that the naphthalene group and the immediate neighbour carbonyls tend to move as a total entity. The motions appear to involve rotations around the nearest oxygen–naphthyl links which are aligned along the main chain axis of polymer. When the neighbouring oxygen–naphthyl links are not co-linear, the rotations about the chain axis will be associated with a crankshaft movement [29]. In this study, the broad β relaxation is observed apparently at ~ 38 °C for the PPO/LCP blends containing high LCP contents (Fig. 11a and b). The β process is observable as a shoulder for the PPO/10 LCP blend. From Fig. 10a and b, the $T_g$ peak of polymer blends is relatively broad due to the difference between the $T_g$ of the LCP and the modified PPO being small. Moreover, it can also be seen that the intensity of the $T_g$ peak decreases dramatically with increasing LCP content. It has been reported that the degree of crystallization of the matrix polymer is increased by the LCP additions [32, 33]. Furthermore, our previous differential scanning calorimetric studies revealed that the heat and degree of crystallization of the matrix polymer are increased by the addition of LCP. This results in the rapid fall in tan delta with LCP content [34]. Because the relaxation associated with $T_g$ is in the amorphous phase, samples with a higher degree of crystallinity tend to exhibit a smaller loss peak. Furthermore, it can also be observed from Figs 10 and 11 that low draw ratio has little effect on the α and β relaxation temperatures.

## 4. Conclusion

The static tensile tests show that a significant improvement in tensile strength was observed at LCP contents

of 10–50 wt % on increasing the draw ratio to 7.9. The improvement in tensile properties is probably due to the reinforcement of the PPO matrix by the LCP fibrils, as observed by the SEM. The modulus of elasticity of polymer blends containing up to 24.32 vol % LCP can be described well with the Tsai–Halpin equation. The dynamic mechanical measurements reveal that the LCP dispersed phase also reinforces the PPO matrix over a wide temperature range but not near the glass transition zone.

## Acknowledgements

This work was supported by a strategic grant (Grant 700-302), City University of Hong Kong. S. L. Liu was on leave from the Institute of Chemistry, Academia Sinica, Beijing 100080, People's Republic of China.

## References

1. A. KOHLI, N. CHUNG and R. A. WEISS, Polym. Eng. Sci. **29** (1989) 573.
2. Y. IDE and Z. OPHIR, *Polym. Eng. Sci.* **23** (1983) 261.
3. D. E. TUREK and G. P. SIMON, *Polymer* **34** (1993) 2750.
4. C. CREVECOEUR and G. GROENINCKX, *Polym. Eng. Sci.* **30** (1990) 532.
5. K. G. BLIZARD, C. FEDERICI, O. FEDERICO and L. CHAPOY, *ibid.* **30** (1990) 1442.
6. A.M. SUKHADIA, A. DATTA and D.G. BAIRD, *Int. Polym. Process* **3** (1992) 218.
7. Y. QIN, D. L. BRYDON, R. R. MATHER and R. H. WARDMAN, *Polymer* **34** (1993) 1202.
8. Q. LIN, J. JHO and A.F. YEE, *Polym. Eng. Sci.* **33** (1993) 789.
9. G. I. TAYLOR, *Proc. R. Soc.* **A146** (1934) 501.
10. K. MIN, J. L. WHITE and J. F. FELLERS, *Polym. Eng. Sci.* **24** (1984) 1327.
11. S. K. BHATTARCHARYA and A. MISRA, *ibid.* **30** (1990) 124.
12. A. K. MITHAL, A. TAYEBI and C.H. LIN, *ibid.* **31** (1991) 1533.
13. A. MEHTA and A. I. ISAYEV, *ibid.* **31** (1991) 971.
14. N. CHAPLEAU, P. J. CARREAU, C. PELETEIRO, P. A. LAVOIE and T.M. MALIK *ibid.* **32** (1992) 1876.
15. S. LI, C. DICKINSON and J. C. W. CHIEN, *J. Appl. Polym. Sci.* **43** (1991) 1111.
16. A. F. YEE, *Polym. Eng. Sci.* **17** (1977) 213.
17. J. STOELTING, F. E. KARASZ and W. J. MacKNIGHT, *ibid.* **10** (1970) 133.
18. P. S. TUCKER, J. W. BARLOW and D. R. PAUL, *Macromolecules* **21** (1988) 1678.
19. A. R. SHULTZ and B. M. BEACH, *ibid.* **7** (1974) 902.
20. T. LIMTASIRI and A. I. ISAYEV, *J. Appl. Polym. Sci.* **42** (1991) 2923.
21. D. E. TUREK, G. P. SIMON, C. TIU, O. T. SIANG and E. KOSIOR, *Polymer* **33** (1992) 4322.
22. B. Y. SHIN, S. H. JANG, I. J. CHUNG and B. S. KIM, *Polym. Eng. Sci.* **32** (1992) 73.
23. S. LEE, S. M. HONG, Y. SEO, T. S. PARK, S. S. HWANG, K. U. KIM and J. W. LEE, *Polymer* **35** (1994) 519.
24. J. C. HALPIN and J. L. KARDOS, *Polym. Eng. Sci.* **16** (1976) 344.
25. L. E. NIELSON, *J. Appl. Polym Sci.* **14** (1970) 4626.
26. J. SARLIN and P. TORMALA, *ibid.* **40** (1990) 453.
27. O. LIN and A. F. YEE, *Polym. Eng. Sci.* **35** (1994) 3463.
28. B. TEKKANAT and R. GIBALA, J. Thermoplastic Compos. Mater. **4** (1991) 190.
29. D. J. BLUNDELL and K. A. BUCKINGHAM, *Polymer* **26** (1985) 1623.
30. R. K. Y. LI, S. LU, C. L. CHOY and C. McCALL, in "Advanced Composites '93", edited by T. Chandra and A. K. Dhingra (The Minerals, Metals and Materials Society, Warrendale, PA 1993) pp. 855–60.
31. M. J. TROUGHTON, G. R. DAVIES and I. M. WARD, *Polymer* **30** (1989) 58.
32 S. K. SHARMA, A. TENDOLKAR and A. MISSA, *Molec. Cryst. Liq. Cryst.* **157** (1988) 597.
33. K. G. BLIZARD and R. R. HAGHIGHAT, *Polym. Eng. Sci.* **33** (1993) 799.
34. S. C. TJONG, S. L. LIU and R. K. Y. LI, *J. Mater. Sci.* **30** (1995) 353.

*Received 19 June 1995*
*and accepted 28 August 1996*